DTU Library

Suppression of reflections by directive probes in spherical near-field measurements

Hansen, Per Christian; Larsen, Flemming H.

Published in:
I E E E Transactions on Antennas and Propagation

Link to article, DOI:
10.1109/TAP.1984.1143286

Publication date:
1984

Document Version
Publisher's PDF, also known as Version of record

Suppression of Reflections by Directive Probes in Spherical Near-Field Measurements

PER C. HANSEN, STUDENT MEMBER, IEEE, AND FLEMMING H. LARSEN, MEMBER, IEEE

Abstract—The influence of probe correction in spherical near-field measurements on signals from outside the test volume is investigated theoretically and experimentally. It is found that the suppression of reflections obtained by a directive probe is not disturbed by the probe correction. A geometric relation between the antenna "minimum sphere" and the probe pattern beamwidth is established, whose satisfaction guarantees the absence of numerical instabilities in the far-field computation. The condition is sufficient, but not necessary if the "minimum sphere" of the antenna is in the near field of the probe.

I. INTRODUCTION

IN THE SPHERICAL near-field far-field technique [1]-[4], the near field is measured on a sphere surrounding the test antenna. Then the far field can be computed in all directions and the directivity can be determined. Often a directive antenna is used as probe, which leads to an amplitude taper over the test aperture so that the field contributions from the outermost parts of the test antenna are attenuated. The probe correction, being a part of the near-field far-field transformation, makes a correction for this effect. Another way of describing the correction is to say that it corrects for the probe measuring a weighted average over the probe aperture rather than the value at a single point.

Probe correction is also applied in planar near-field measurements [5]. Here, the correction can be regarded as a division of the Fourier-transformed measured data by the radiation pattern of the probe. Hence, the correction tends to amplify the test antenna pattern in directions away from boresight. In the presence of error signals and noise this can lead to large errors in the null directions of the probe.

In the spherical technique there is no similar simple interpretation of the probe correction. Since the signals from current elements away from the center of the test volume are attenuated by the probe pattern, these signals must be amplified by the probe correction. For instance the sidelobes of a reflector antenna are raised by the correction [6]. One could think that spurious signals from the surroundings outside the test volume could also be amplified as in the planar technique. The question of how the probe correction treats these error signals is the subject of a M.Sc. thesis [7] and the present paper.

II. EXPERIMENTAL STUDY OF REFLECTIONS

In the experimental part of our investigation we have performed a series of measurements at 11.7 GHz with the spherical scanner in the radio anechoic chamber at the Technical University of Denmark. The near field of a 30 λ reflector antenna was measured and transformed to the far field by use of the program SNIFTC [8]. In order to study the influence of probe directivity two probes were used: a 15 dB gain conical horn and an open-ended circular waveguide with a gain of approximately 5 dB. Corrections for the probe patterns were included in the transformations.

The spherical scanner geometry is shown in Fig. 1. The probe is fixed while the test antenna is rotated in θ and ϕ. We inserted a 1 m × 2 m aluminum plate into the anechoic chamber with the middle of the plate at the same height as the probe and test antenna, so that a large reflected error field was produced.

In the near field (not shown here), the directive probe obviously gives the best suppression of the reflected error signal; but it is not obvious that this also applies to the transformed and probe-corrected far field. Fig. 2(a) shows the far field without reflections, while Figs. 2(b) and 2(c) show the far fields when the large reflection is introduced, giving rise to a large lobe at $\theta = 50°$. The directive probe pattern is 13 dB below the pattern of the waveguide probe in the direction of specular reflection, and by comparing Figs. 2(b) and 2(c) we see that this suppression of the reflection in the near field is maintained in the far field. The probe correction amplifies the lobes generated by currents inside the test antenna volume and away from center [9], but it does not amplify the error signals. Thus the directive probe yields the best suppression of the reflections.

A series of computer simulations of different measurement situations has been carried out, and the simulations confirm the experimental results [7].

III. THEORETICAL COMPARISON OF PROBE CORRECTIONS

In the planar technique the probe correction mechanism is normally described as a "division" of the measured and Fourier-transformed data by the radiation pattern of the probe. Although the cylindrical and spherical probe corrections are not as simple as this, we have established an analogy between the probe corrections in the three techniques.

First, let us give a brief summary of the planar technique as described by Kerns [5]. Introducing the transverse displacement of the probe $\mathbf{P} = x\mathbf{e}_x + y\mathbf{e}_y$, the received signal in the probe is

$$b_0'(\mathbf{P}) = a_0 \int e^{i\mathbf{K}\cdot\mathbf{P}} \mathbf{S}_{02}'(\mathbf{K}) \cdot \mathbf{S}_{10}(\mathbf{K}) e^{i\gamma d}\, d\mathbf{K} \tag{1}$$

where $\mathbf{K} = k_x\mathbf{e}_x + k_y\mathbf{e}_y$ is the index parameter for the plane wave expansion. $\mathbf{S}_{02}'(\mathbf{K})$ is the receiving characteristic of the probe, and $\mathbf{S}_{10}(\mathbf{K})$ is the wanted transmitting characteristic of the test antenna. Both of these are two-component vectors, and for each $\mathbf{K}$, the two components correspond to two orthogonal polarizations. Equation (1) represents a Fourier transformation, and by inversion we obtain

$$\mathbf{S}_{02}'(\mathbf{K}) \cdot \mathbf{S}_{10}(\mathbf{K}) = \frac{e^{-i\gamma d}}{4\pi^2 a_0} \int b_0'(\mathbf{P}) e^{-i\mathbf{K}\cdot\mathbf{P}}\, d\mathbf{P}. \tag{2}$$

Manuscript received February 18, 1983; revised August 26, 1983.

P. C. Hansen is with the Institute for Numerical Analysis, Bldg. 303, Technical University of Denmark, DK-2800 Lyngby, Denmark.

F. H. Larsen is with the Electromagnetics Institute, Bldg. 348, Technical University of Denmark, DK-2800 Lyngby, Denmark.

0018-926X/84/0200-0119$01.00 © 1984 IEEE

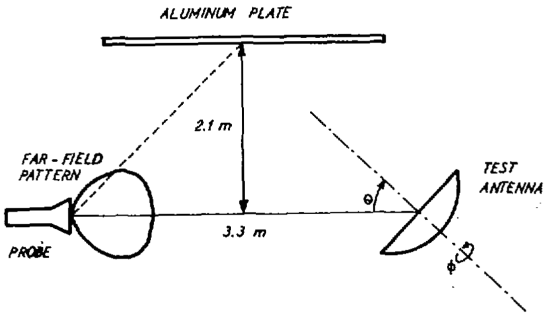

Fig. 1. Spherical near-field measurement geometry with reflecting plate (top view).

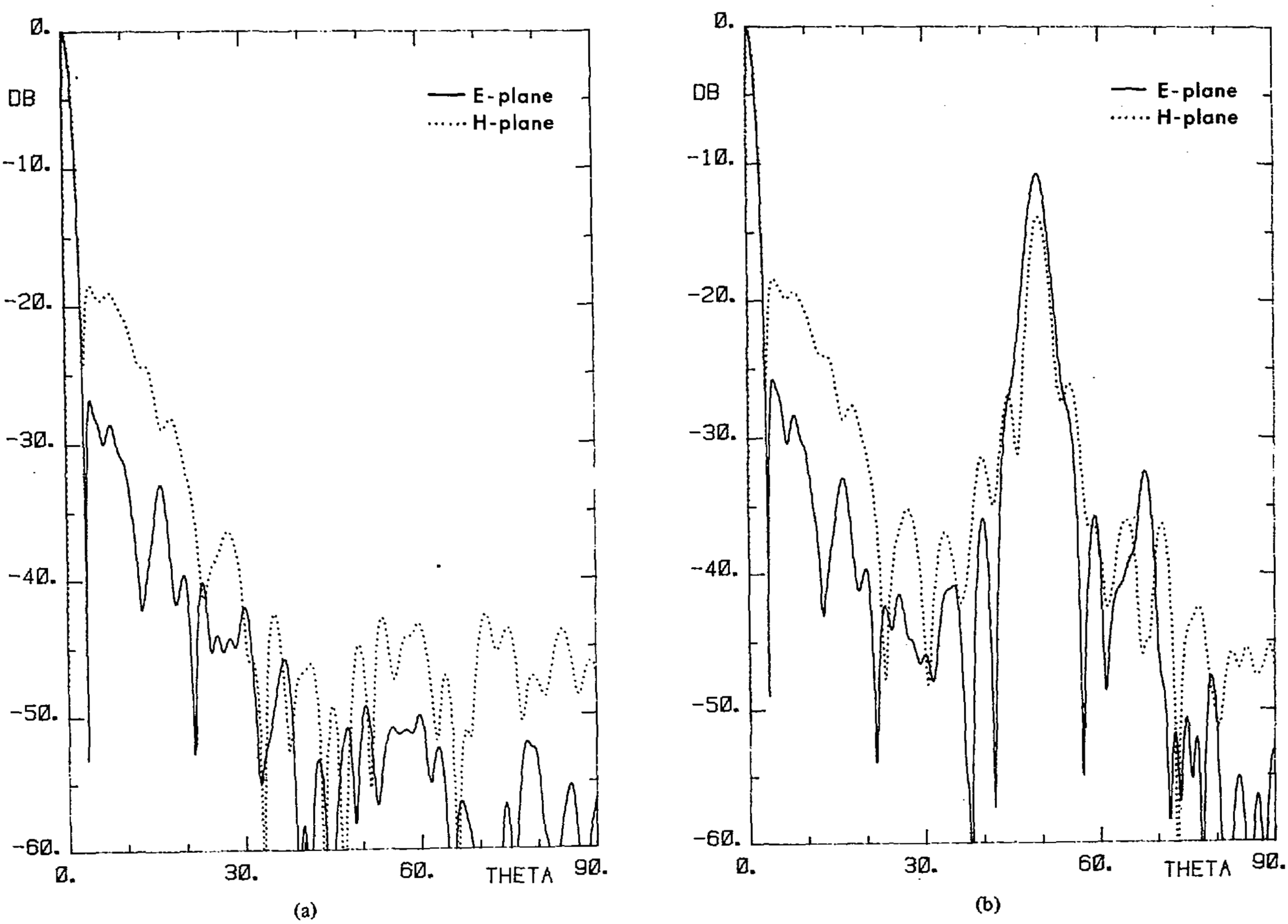

Fig. 2. Far field of 30 λ reflector antenna computed from measured near-field data illustrating the suppression of reflected signals. (a) 15 dB probe, no reflecting plate. (b) 5 dB probe, with reflecting plate. (c) 15 dB probe, with reflecting plate.

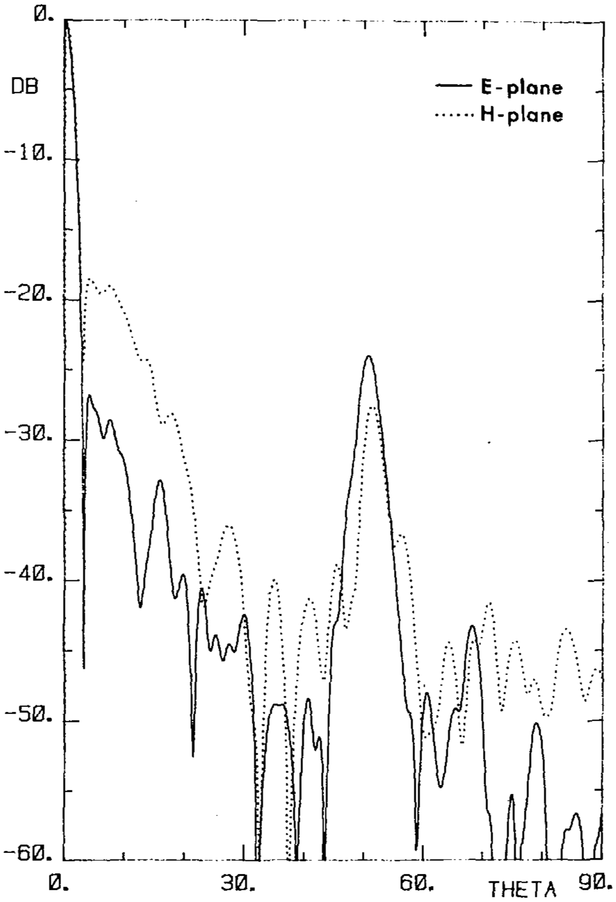

(c)

Fig. 2. (*continued*)

Equation (2) yields one equation with two unknowns. Hence, one must apply a second probe or the same probe rotated 90° to obtain a second equation. Then for each $\mathbf{K}$ one can solve the system of two linear equations for $\mathbf{S}_{10}(\mathbf{K})$. The right side is computed independently of the probe pattern, and the probe correction enters through the coefficients $\mathbf{S}'_{02}(\mathbf{K})$ which actually are the probe receiving patterns as a function of $\mathbf{K}$.

The probe correction concept for nonplanar scanning was originally introduced by Brown and Jull in a paper [10] on two-dimensional cylindrical scanning. The field component E_z from the test antenna is expanded in a discrete spectrum:

$$E_z(r, \theta) = \sum_{n=-\infty}^{\infty} a_n H_n^{(2)}(\beta r) \exp(jn\theta) \tag{3}$$

where a_n are the expansion coefficients and $H_n^{(2)}(\beta r)$ are cylindrical Hankel functions. The received signal P in the probe is expressed as a summation over the cylindrical modes:

$$P(\theta) = \sum_{n=-\infty}^{\infty} c_n(b)\, a_n \exp(jn\theta) \tag{4}$$

which by Fourier transformation yields

$$a_n c_n(b) = \frac{1}{2\pi} \int_0^{2\pi} P(\theta) \exp(-jn\theta)\, d\theta. \tag{5}$$

Brown and Jull introduced the term response constants for $c_n(b)$ expressing the probe's sensitivity to the test antenna modes at the measuring radius b. Probe correction enters the computation of the expansion coefficients a_n through the division of the measured and Fourier-transformed data by the response constants $c_n(b)$, which depend on the probe pattern and b.

Also in the three-dimensional spherical technique [9] a discrete spectrum arises

$$\mathbf{E}(r, \theta, \phi) = \sum_{s=1}^{2} \sum_{n=1}^{\infty} \sum_{m=-n}^{n} Q_{smn} \mathbf{F}_{smn}(r, \theta, \phi) \tag{6}$$

in which Q_{smn} are the expansion coefficients with indices (s, m, n), where $s = 1$ for transverse electric (TE) modes and $s = 2$ for transverse magnetic (TM) modes. The $\mathbf{F}_{smn}(r, \theta, \phi)$ are spherical wave functions as defined in [4]. The signal received by the probe in a spherical near-field measurement is expressed as

$$W(A, \phi, \theta, \chi) = \sum_{smn\mu} Q_{smn} e^{im\phi} d^n_{\mu m}(\theta) e^{i\mu\chi} P_{s\mu n}(A) \tag{7}$$

where W is the signal received in position (θ, ϕ) at the measurement radius A and with χ describing the polarization angle of the probe. $e^{im\phi} d^n_{\mu m}(\theta) e^{i\mu\chi}$ are rotation coefficients of the spherical wave functions, and $P_{s\mu n}(A)$ are spherical response constants, corresponding to $c_n(b)$ above. They express the probe's sensitivity to the test antenna modes at the measuring radius A in the position $(\phi, \theta, \chi) = (0, 0, 0)$.

The probe is assumed to be sensitive to modes with $\mu = \pm 1$ only. Therefore, when orthogonality relations are applied to both sides of (7), a system of two linear equations is obtained

$$\begin{bmatrix} P_{11n}(A) & P_{21n}(A) \\ P_{1,-1,n}(A) & P_{2,-1,n}(A) \end{bmatrix} \begin{bmatrix} Q_{1mn} \\ Q_{2mn} \end{bmatrix} = \begin{bmatrix} (\Delta\Pi W)^n_{1m} \\ (\Delta\Pi W)^n_{-1,m} \end{bmatrix} \tag{8}$$

in which

$$(\Delta\Pi W)^n_{\mu m} = \frac{n + 1/2}{4\pi^2} \int_{\chi=0}^{2\pi} \int_{\phi=0}^{2\pi} \int_{\theta=0}^{\pi} W(A, \phi, \theta, \chi) \cdot d^n_{\mu m}(\theta) \sin\theta\, d\theta e^{-im\phi}\, d\phi e^{-i\mu\chi}\, d\chi. \tag{9}$$

Again the integrals on the right side of (8) are computed independently of the probe pattern, and each pair of expansion coefficients (Q_{1mn}, Q_{2mn}) is the solution to a system of two equations with two unknowns. Then the far field can be evaluated by use of (6) with $r = \infty$ or (7) with $A = \infty$.

Comparing the three techniques we see that what they have in common is that some integral transformation is applied to the measured data, and this transformation separates the contributions to each pair of modes. The integral transformation is independent of the probe pattern as pointed out by Wacker [3]. Thus the process of solving the equations, in which the response constants are coefficients, compensates for

1) the measurement distance;
2) the probe pattern.

Probe correction only implies that different response constants are applied for different probes. Hence, one might say that the solution of the expansion-coefficient equations (2), (5), and (8) makes the near-field measurement plus transformation equally sensitive to all of the modes (planar, cylindrical or spherical waves, respectively).

If, for certain modes, the response constants are small in amplitude, the determination of the corresponding expansion coefficients becomes unstable. In the planar technique each pair of expansion coefficients and each pair of response constants (for the test antenna and the probe, respectively) is associated with a single far-field direction. Therefore the instabilities are associated with nulls in the probe pattern and they are confined to distinct directions in the computed far field. For nonplanar expansions, instabilities will occur for certain modes only, and in the far field the mode fields and hence the errors will generally contribute in all directions.

IV. INVESTIGATION OF THE SPHERICAL RESPONSE CONSTANTS

In this section the spherical response constants are computed for various probes in order to identify possible instabilities in the spherical probe correction.

First we shall note some properties of the spherical wave functions $\mathbf{F}_{smn}$ necessary for interpretation of the results. The maximum mode index $n_{\max}$ in the spherical wave expansion for the field excited by the test antenna is approximately kr_0, where r_0 is radius of the smallest sphere (minimum sphere) surrounding the antenna. Further, a mode with index n can only be excited by an antenna with $r_0 > n/k$. Therefore we can also use the term minimum sphere in connection with a single spherical wave, and in the near-field to far-field transformation one only needs to calculate response constants for $n \leqq n_{\max}$. Likewise, the maximum mode index $\nu_{\max}$ for the probe coefficients $P_{\sigma\mu\nu}$ is determined by the size of the probe.

The response constants are computed by the formula:

$$P_{s\mu n}(A) = \frac{1}{2} \sum_{\sigma\nu} C^{sn}_{\sigma\mu\nu}(A) P_{\sigma\mu\nu} \tag{10}$$

where $C^{sn}_{\sigma\mu\nu}(A)$ are translation coefficients used when expressing the test antenna modes $\mathbf{F}_{s\mu n}$ in terms of modes $\mathbf{F}_{\sigma\mu\nu}$ in the probe coordinate system. $P_{\sigma\mu\nu}$ are receiving coefficients for the probe in its own coordinate system.

In spherical near-field measurements a conical horn excited by a TE_{11} mode in a circular waveguide is used as probe, and hence $P_{\sigma\mu\nu}$ and $P_{s\mu n}(A)$ are nonzero for $\mu = \pm 1$ only. Usually the probe is approximately linearly polarized in the E- and H-planes. For such a probe, the matrix in (8) is nearly orthogonal, and the solution process is well conditioned. With the additional requirement that the E-plane pattern is the same as the H-plane pattern such that the polarization is the same as that of a Huygens source, the matrix takes the form [6]:

$$\begin{bmatrix} P_{11n}(A) & P_{21n}(A) \\ P_{1,-1,n}(A) & P_{2,-1,n}(A) \end{bmatrix} = \kappa_n(A) \begin{bmatrix} 1 & 1 \\ 1 & -1 \end{bmatrix} \tag{11}$$

and the condition number of the matrix is one. Our investigation is therefore concerned with the variation of $|\kappa_n(A)|$ as a function of n, A, and probe directivity.

Two probes have been modelled as linear endfire arrays of Huygens sources, c.f. Table I. These probes have been used because each Huygens source measures a combination of E- and H-field components so that the received signal in the simulations can be calculated exactly as a weighted sum over the array elements. The receiving patterns of the two probes are shown in Fig. 3, and a series of curves of $|\kappa_n(A)|$ for the two probes is shown in Figs. 4(a)-(f).

When the measurement range approaches infinity (corresponding to far-field measurements), all spherical modes tend to appear as plane waves with axial incidence on the probe. This means that the variation of $|\kappa_n(A)|$ with n follows the amplitude of the individual modes on the z-axis. Our mode functions $\mathbf{F}_{smn}$ are normalized so that the radiated power for each mode is $1/2\,|Q_{smn}|^2$ [4], and for $|m| = 1$ they satisfy

$$|kr\mathbf{F}_{smn}| \to \frac{k}{\sqrt{\eta}} \sqrt{\frac{2n+1}{16\pi}}, \quad \text{for } kr \to \infty \tag{12}$$

where η is the free space admittance. Accordingly, the two curves in Fig. 4(f) are proportional to $\sqrt{2n+1}$. The difference between the curves is equal to the ratio of boresight gain for the two probes.

At a finite distance the probe will still be in the far field of the low order modes, i.e., for $n^2 < kA$. Hence the $\sqrt{2n+1}$ variation dominates the left parts of Figs. 4(a)-4(e).

In the right parts of Figs. 4(a) and 4(b) the curves increase dramatically. Mathematically this is due to the spherical Hankel functions $h_p^{(2)}(kA)$ in the translation coefficients $C^{sn}_{\sigma\mu\nu}(A)$. Hankel functions of order p up to $n + \nu_{\max}$ are included and for $p > kA$ these functions become large. Physically, $n_{\max} + \nu_{\max} > kA$ implies that the minimum spheres of the test antenna and the probe intersect. This situation should be avoided in practical measurements. On the other hand large response constants imply that the mode contributions will be heavily attenuated in the near-field far-field transformation. Thus they will not cause instabilities in the computations, unless one transforms from the measurement distance to a shorter distance. Here, there is a danger of overflow during the computation of the response constants.

For most of the curves we observe some "nulls" indicating

TABLE I
DATA FOR THE TWO PROBES, MODELLED AS LINEAR ENDFIRE ARRAYS OF HUYGENS SOURCES

Directivity	15 dB	21 dB
Length	1.25 λ	3.60 λ
Number of elements	6	13
$\nu_{\max}$	14	25

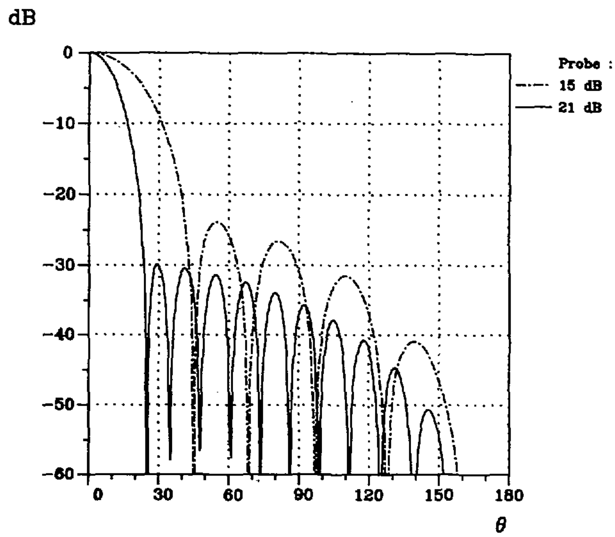

Fig. 3. Far-field radiation patterns for the probes specified in Table I.

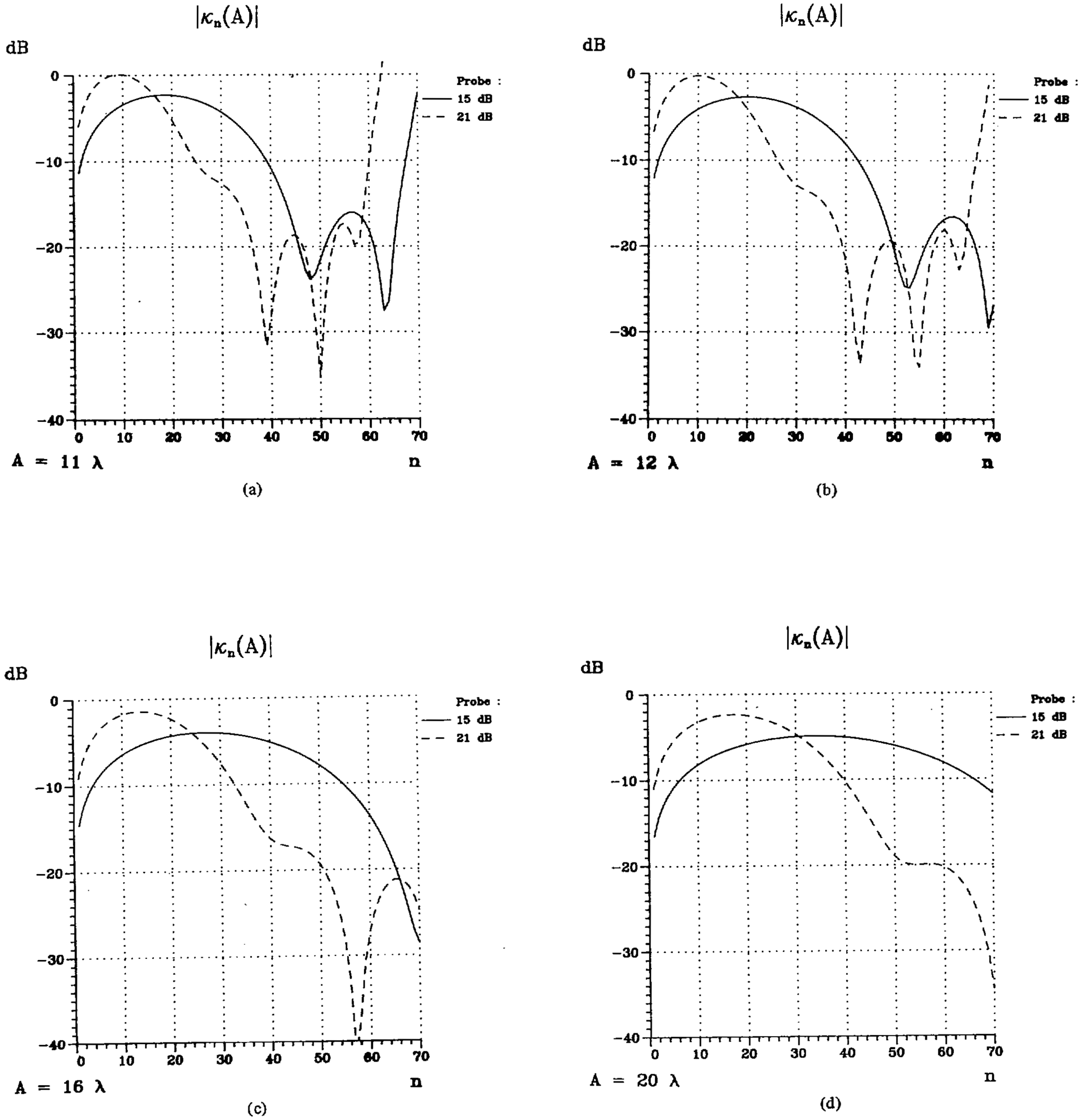

Fig. 4. Graphs of the response constants $|\kappa_n(A)|$ for the two probes specified in Table I at various distances.

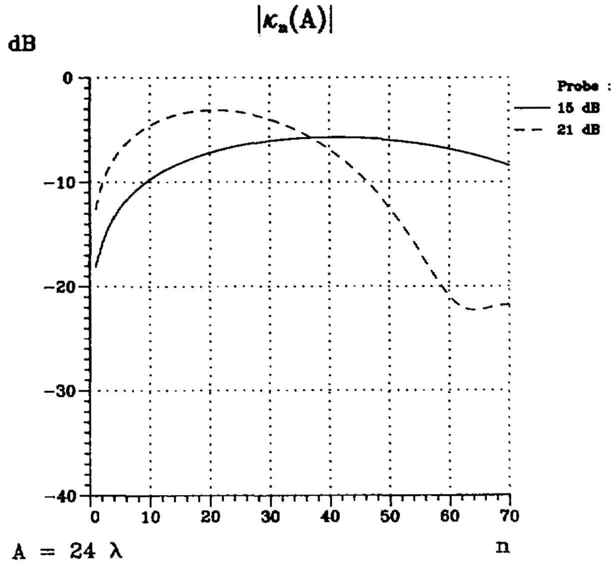

(e)

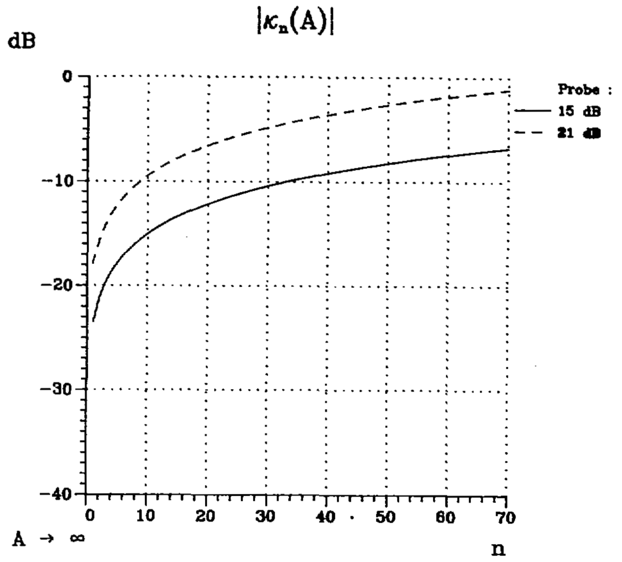

(f)

Fig. 4. (*continued*)

that the probe is insensitive to particular modes. The major feature of the Hankel functions for $kr < n^2$ is that the phase variation with r is less than 2π per wavelength. To a first approximation the mode field can be described as having an angle of incidence u to the probe axis, different from zero. Using an asymptotic expression for the phase variation [11, eq. (9.2.29)] one can calculate the radial component of the propagation vector:

$$k_r = \frac{d\theta_{n+1/2}}{dr} \cong \left(1 - \frac{n(n+1)}{2(kr)^2}\right) k \tag{13}$$

and get the following expression for the angle on incidence:

$$u = \sin^{-1} \sqrt{1 - \left(\frac{k_r}{k}\right)^2} \cong \sin^{-1} \frac{\sqrt{n(n+1)}}{kA}. \tag{14}$$

The above expression is close to the incidence angle of a ray from the edge of the minimum sphere given in Fig. 5.

When u is calculated from (n, A) corresponding to the first null of the curves for the 15 dB probe in Figs. 4(a), 4(b), and 4(c), we get 44.6°, 44.1°, and 44.5°, respectively. This is very close to the angle of the first null in the radiation pattern of the 15 dB probe, c.f. Fig. 3. Similarly, the other nulls in Figs. 4(a)-4(d) correspond to nulls in the probe patterns in Fig. 3.

For probe corrected cylindrical near-field measurements, Borgiotti [12], [13] has shown that if the test antenna can be assumed to be in the far field of the probe, then the response constants can be calculated by a saddle point integration and each response constant will depend on the probe pattern in one direction only. Because of the appearance of a Legendre function in the formulas for the spherical waves, a similar derivation has not been possible in the spherical case; but Figs. 4(a)-4(e) illustrate that the probe receiving patterns via the concept of incidence angle are reflected in the curves for the response constants. Only, the first null of the 21 dB probe changes to a "shoulder" in the $|\kappa_n(A)|$ curves. As long as the minimum sphere of the test antenna lies within the main beam of the probe, instabilities will show up for $n > n_{\max}$ only.

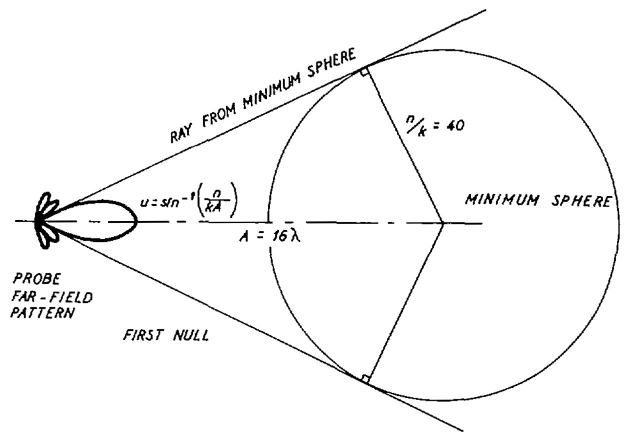

Fig. 5. Illustration of the correspondence between minimum sphere of a mode and angle of incidence. The specific geometry corresponds to Fig. 4(c) and the 21 dB probe.

The disappearance of the first null for the 21 dB probe is caused by the distance to the minimum sphere of the corresponding modes (i.e., $A - n/k$) being smaller than the far-field distance of the probe. Thus the response constants are related to the probe pattern at the actual measurement distance rather than the far-field pattern. Computer simulations have verified that especially the first null tends to vanish at short distances. As an example, Fig. 5 corresponds to Fig. 4(c) for the 21 dB probe. The first null at $\theta = 25°$ would imply that only a sphere up to $n_{\max} = 38$ could be used. However, since the first null has disappeared at this distance, antennas with $n_{\max}$ up to 50 can be measured. In the extreme situation where the probe is larger than the test antenna, the situation is similar to a compact range measurement in which the far field is measured directly, and the response constants will therefore follow the curves in Fig. 4(f) without instabilities.

Summarizing, we have verified the existence of instabilities for the probe correction in the spherical technique, where error signals and noise could introduce errors in the computed far field. Such errors would arise through amplification of certain critical modes and generally be "spread out" over the entire angular space. However, as long as the probe illuminates the entire minimum sphere of the test antenna, the instabilities appear outside the mode range necessary to represent the test antenna field. Errors can therefore be avoided by proper truncation of the expansion for the test antenna field. Further, since the response constants are always computed as a part of a far-field transformation, instabilities can be detected in the computer program.

V. CONCLUSION

In spherical near-field measurements a directive probe increases the direct signals from the test antenna and suppresses reflected signals from outside the test antenna volume. The probe correction in the subsequent data processing compensates for the probe pattern variation over the test antenna aperture. Theoretical investigations have shown that numerical instabilities may arise for certain critical modes. However, as long as the probe illuminates the entire test antenna volume, these instabilities will correspond to directions from outside the test antenna. Accordingly, they can be avoided by proper truncation of the spherical wave expansion for the test antenna field. Measurements have verified that signals received from the surroundings will not be amplified by the probe correction.

It should be emphasized that the results above do not apply to multiple reflections between the test antenna and the probe. In general these reflections will increase with increasing size of the probe, and this effect can in some cases put a limit on the feasible probe size.

ACKNOWLEDGMENT

The authors are indebted to Professor Jesper E. Hansen, who supervises the research program on spherical near-field measurements at the Technical University of Denmark.

REFERENCES

[1] F. Jensen, "Electromagnetic near-field—far-field correlations," Ph.D. dissertation, Lab. Electromagn. Theory, Tech. Univ. Denmark, Rep. LD 15, July 1970.
[2] ——, "On the probe compensation for near-field measurements on a sphere," *Archiv für Elektronik und Übertragungstechnik,* vol. 29, no. 7/8, pp. 305–308, July/Aug. 1975.
[3] P. F. Wacker, "Non-planar near-field measurements: Spherical scanning," Electromagn. Div., Inst. Basic Stand., Nat. Bur. Std., Boulder, CO, Rep. NBSIR 75-809, July 1975.
[4] F. H. Larsen, "Probe-corrected spherical near-field antenna measurements," Ph.D. dissertation, Electromagn. Inst., Tech. Univ. Denmark, Rep. LD 36, Dec. 1980.
[5] D. M. Kerns, "Plane wave scattering-matrix theory of antennas and antenna-antennas Interactions," U.S. Dept. Commerce, Nat. Bur. Std., Boulder, CO, NBS Monograph 162, June 1981.
[6] E. L. Christensen, J. E. Hansen, C. K. Hansen, S. B. Hansen, F. H. Larsen and G. H. Lemanczyk, "Experimental spherical near-field antenna test facility, phase 2," Final Rep., ESA Contract 3916/79/NL/DG, Electromagn. Inst., Tech. Univ. Denmark, R 248, Dec. 1981.
[7] P. C. Hansen, "Influence of probe directivity in spherical near-field measurements," (in Danish), M.Sc. Thesis, Electromagn. Inst., Tech. Univ. Denmark, Jan. 1982.
[8] F. Holm Larsen, "SNIFTC. Spherical near-field transformation program with probe correction. Manual," Electromagn. Inst., Tech. Univ. Denmark, Rep. R 201, Oct. 1978.
[9] F. Holm Larsen, "Probe correction of spherical near-field measurements," *Electron. Lett.*, vol. 13, no. 14, pp. 393–395, July 1977.
[10] J. Brown and E. V. Jull, "The prediction of aerial patterns from near-field measurements," *Proc. Inst. Elec. Eng.*, vol. 108B, paper 3649E, pp. 635–644, Nov. 1961.
[11] M. Abramowitz and I. A. Stegun, *Handbook of Mathematical Functions*. New York: Dover, 1965.
[12] G. V. Borgiotti, "Integral equation formulation for probe corrected far-field reconstruction from measurements on a cylinder," *IEEE Trans. Antennas Propagat.*, vol. AP-26, no. 4, pp. 572–578, July 1978.
[13] F. H. Larsen, "Comments on Integral equation formulation for probe corrected far-field reconstruction from measurements on a cylinder," *IEEE Trans. Antennas Propat.*, vol. AP-27, no. 6, pp. 897–898, Nov. 1979.

Per C. Hansen (S'83) was born in Nyborg, Denmark, on July 9, 1957. He received the M.Sc. degree in electrical engineering from the Technical University of Denmark, Lyngby, in 1982. Currently, he is working toward a Ph.D. degree at the Institute for Numerical Analysis, Technical University of Denmark.

His research concerns the application of singular value decomposition to algebraic problems with nonunique solutions.

Flemming H. Larsen (M'74) was born in Copenhagen, Denmark, on March 10, 1948. He received the M.Sc. and Ph.D. degrees in electrical engineering from the Technical University of Denmark, Lyngby, in 1973 and 1982, respectively.

From 1973 to 1974 he worked on tropospherical duct propagation, partly at the Danish Defence Research Establishment and partly at Electromagnetics Institute, Technical University of Denmark, Lyngby. Since 1975 he has been a Research Associate at The Electromagnetics Institute, Technical University of Denmark, participating in the development of a spherical near-field measurement system for the European Space Agency. As a specialist in near-field antenna measurements, he is currently a consultant to TICRA A/S, Copenhagen, Denmark.